HHS Public Access

Author manuscript

*Magn Reson Med*. Author manuscript; available in PMC 2019 September 01.

Published in final edited form as:

*Magn Reson Med*. 2018 September ; 80(3): 1036–1047. doi:10.1002/mrm.27100.

# Placental Perfusion Imaging Using Velocity-Selective Arterial Spin Labeling

**Zungho Zun, PhD**[1,2,3,4] and **Catherine Limperopoulos, PhD**[1,2,3,4]

[1]Division of Diagnostic Imaging and Radiology, Children's National Medical Center, Washington, DC, United States

[2]Division of Fetal and Transitional Medicine, Children's National Medical Center, Washington, DC, United States

[3]Department of Pediatrics, School of Medicine and Health Sciences, George Washington University, Washington, DC, United States

[4]Department of Radiology, School of Medicine and Health Sciences, George Washington University, Washington, DC, United States

## Abstract

**Purpose—**The placenta remains the least understood human organ in large part because of the lack of non-invasive tools currently available to examine placental function in vivo. This study investigates the feasibility of using velocity-selective arterial spin labeling (VSASL) to assess placental perfusion.

**Methods—**In placental perfusion imaging, VSASL was compared with pseudocontinuous ASL (PCASL), which is currently the standard technique in brain ASL. Reproducibility of placental VSASL was evaluated using two repeated scans within the same imaging session. Inflow-dependence of placental VSASL was investigated by modulating VSASL signal using maternal inhalation of 100% oxygen and variation of cutoff velocity. All experiments were performed in healthy pregnant volunteers at 1.5 T.

**Results—**Apparent placental perfusion measured using PCASL with two different labeling locations was only 16% and 9% of that of VSASL (n=7, $p<0.01$ for both). Placental VSASL was highly reproducible based on within-subject coefficient of variation of 3.5%, repeatability of 19.7 ml/100 g/min, and intraclass correlation coefficient of 0.97 (n=14). Placental VSASL was also found to be dependent on blood inflow given that the absolute change in apparent placental perfusion with maternal hyperoxia was significantly larger than that of two repeated scans under normoxia (n=7, $p<0.01$) and there was a significant difference in apparent placental perfusion between different cutoff velocities (n=6, $p<0.01$).

**Conclusion—**This study demonstrates the feasibility of non-invasive placental perfusion imaging using VSASL and lays the groundwork for acquiring placental perfusion images in pregnancies at high risk where placental function is impaired.

Corresponding Author: Zungho Zun, Children's National Medical Center, 111 Michigan Ave, NW, Washington, DC 20010, Phone: (202) 476-5951, zzun@childrensnational.org.

**Keywords**

placental perfusion; arterial spin labeling; velocity-selective arterial spin labeling; ASL; VSASL

## Introduction

The placenta plays a central role for fetal growth and development during pregnancy. Placental dysfunction is the most common cause of prevalent conditions affecting the viable fetus such as fetal growth restriction (FGR) and preeclampsia (1-4). Screening and diagnosis of these disorders, however, currently relies on indirect measures to the placenta in large part due to the lack of non-invasive tools to examine and monitor placental function in vivo. This in turn limits sensitivity and predictive validity of the current examination methods and complicates early and reliable detection of abnormal placental function, which is critical to open therapeutic windows currently unavailable in high-risk pregnancies complicated by placental dysfunction.

Arterial spin labeling (ASL) is a non-invasive, powerful imaging method for measuring tissue perfusion, and has extensively been applied in the brain for measurement of cerebral blood flow (CBF) (5). While conventional perfusion MRI techniques require the use of contrast agents, which are contraindicated during pregnancy, ASL utilizes the water molecules in arterial blood as an endogenous contrast agent, making it optimal for examining placental perfusion in pregnancy. Currently, pseudocontinuous ASL (PCASL) is the standard labeling method in the brain due to its highest signal-to-noise ratio (SNR) among existing ASL methods (6). For the organs outside of the brain such as the kidney, lung, and heart, flow-sensitive alternating inversion recovery (FAIR) (7,8) has often been the labeling method of choice especially in feasibility studies with single slice imaging because there is no need to determine the labeling region in this method in the presence of complicated arterial path (9-11).

Application of ASL in the placenta faces several challenges. The biggest challenge in placental ASL would be to determine the optimal labeling region. This arises from the complex path of arterial blood flow to the placenta, which mainly follows the circuitous route of the descending aorta, internal iliac arteries, and uterine arteries. In addition, there is another route from the descending aorta to the ovarian arteries, which accounts for 15% of placental perfusion (12). Using conventional ASL approaches, it may be difficult to find a labeling region that has high labeling efficiency and includes all these contributions of blood flow to the placenta unless labeling is placed in the descending aorta. This in turn would be too far from the placenta, leading to significant reduction of SNR due to $T_1$ decay of the label during prolonged arterial transit delay. Second, relatively large blood volume of the placenta [approximately 50% (13)] may confound quantification of placental perfusion. Because the small extravascular space likely incurs short mean transit time (MTT) of the labeled water in the placenta, placental perfusion may be miscalculated using conventional ASL methods based on the assumption of no clearance/transition of the label from each tissue voxel (14), which is required in the presence of inhomogeneous arterial transit delay. Although global placental perfusion (i.e. mean perfusion of all voxels within the placenta)

may represent correct perfusion values of the whole placenta, regional perfusion measures, that likely retain important information, may become erroneous due to this transition of the label from one voxel to another with short MTT. A similar issue has been demonstrated previously in the application of ASL in the lung, which is another human organ with short MTT due to limited water exchange between intra- and extravascular spaces (15). While these two challenges will be resolved or less problematic with single-slice ASL, single-slice coverage in turn limits its clinical usage. Lastly, placental ASL requires correction for placental motion primarily caused by maternal breathing. Motion artifacts in ASL may be overcome with the use of motion-resistant image readout and/or excellent background suppression across a wide range of $T_1$ values. In 2D single-shot ASL, retrospective motion correction is also possible using registration of ASL images with no (or deliberately suboptimized) background suppression; however, ASL with non-rigid body registration has never been demonstrated in prior studies.

To date, very few studies attempted placental ASL in humans. The first placental ASL was reported about twenty years ago from a group that published three subsequent studies using presumably the same imaging sequence based on FAIR labeling and a Look-Locker imaging scheme at 0.5 T (16-18). While the authors showed reasonable placental perfusion measures in their preliminary data, the suboptimal ASL imaging protocol with low SNR and single-slice imaging coverage failed to demonstrate adequate ASL image quality and a significant difference in placental perfusion between low- and high-risk pregnancies. More recently, a study reported placental ASL using FAIR labeling with a single inversion time at 1.5 T, which is a more optimized ASL approach for humans. However, this study presented an analysis of ASL difference signal only, without absolute perfusion quantification (19).

Recently, we have reported placental perfusion measures in pregnancies complicated by fetal congenital heart disease (CHD) as well as healthy pregnancies using velocity-selective ASL (VSASL), and have demonstrated a significant difference in placental perfusion between the two cohorts (20). VSASL was originally developed for brain ASL to correct for errors of conventional ASL in the presence of slow or delayed blood flow (21,22). However, we propose that VSASL is also well suited for the placenta because VSASL effectively addresses the aforementioned challenges of placental ASL. In this method, labeling of arterial blood is achieved based on its velocity regardless of location. As such, measurement error due to long arterial transit delay can be minimized and all contributions of blood flow into the placenta (even the contribution from fetal side) are reflected in the measurement without having to determine the labeling region. VSASL also provides uniform arterial transit delay, which is zero in principle, and this leads to more accurate assessment of placental perfusion compared to conventional ASL methods in the presence of presumably short MTT in the placenta. Furthermore, our image acquisition is effective for reducing motion artifacts. The spiral-based image acquisition of our method is intrinsically less susceptible to motion. Accurate background suppression that is extremely useful for reducing physiological noise due to subject motion can be achieved only with 3D image acquisition because in 2D multislice imaging, background suppression can be optimized only for one target slice. In this study, we demonstrate the feasibility of applying VSASL in the human placenta and evaluate its performance for placental perfusion measurements. To this end, we compare VSASL against PCASL in the placenta, evaluate reproducibility of

placental VSASL, and demonstrate inflow-dependence of placental VSASL to confirm that observed VSASL signal reflects blood flow.

## Methods

### Pulse Sequence

VS labeling was achieved using dual hyperbolic secant (sech) inversion as described in Ref. 21. Cutoff velocity was set to 2 cm/s, and velocity-encoding gradients were applied in the S/I direction with Gmax = 14 mT/m, which avoids significant errors from eddy current in VSASL (23,24). The second velocity-encoding for eliminating blood flow higher than the cutoff velocity from the ASL images was applied immediately prior to image acquisition. Inflow time (TI) of 1600 ms was used. Background suppression was obtained using one global saturation and four sech inversion pulses that were applied 2100, 1583, 825, 312, and 81 ms prior to image acquisition, respectively. This combination of sequence timing was found using the optimization process that considered relaxation effects of not only $T_1$ but also $T_2$ of static tissues, because $T_2$ decay during VS labeling pulse (duration = 21 ms) was non-negligible. Signal attenuation from diffusion effect of VS labeling pulse is expected to be up to 0.08% of $M_O$ (equilibrium magnetization) in the placenta based on the b-value of 0.34 s/mm$^2$ of our current pulse sequence and the reported apparent diffusion coefficient (ADC) values of the human placenta, which is in a range of 0.001–0.0024 mm$^2$/s (25-27). This is negligible compared to ASL signal of 5.6% of $M_O$, based on our placental VSASL scans in healthy pregnant women (20). Image acquisition was performed using fast-spin-echo 3D stack of spirals with 8 interleaves in the axial orientation. Imaging parameters included TR/TE = 2615/10 ms, FOV = 36–50 cm, matrix size = 64 × 64, number of slices = 36–44, and slice thickness = 4 mm. ASL imaging with NEX = 5 was followed by proton-density imaging, which was performed using saturation recovery with the same image readout as ASL imaging. Measured proton-density signal was corrected for the effect of $T_1$ relaxation. Total scan time of placental VSASL was 3:55 min. 2D $T_2$-weighted single-shot fast spin echo imaging was also performed for anatomical imaging

### Reconstruction

ASL images were reconstructed using sensitivity encoding (SENSE) (28) with the reduction factor R=1, (also known as optimal B1 reconstruction) to optimally combine complex signal from all coil elements even when signal is close to zero (9,29,30). Coil sensitivity maps were generated from proton-density images. All reconstruction process was performed using customized MATLAB (MathWorks Inc., Natick, MA) scripts.

### Quantification

ASL quantification of placental perfusion $f$ (in unit of ml/100 g/min) was performed based on the following equation modified from Buxton's general kinetic model (14).

$$f = \frac{(C - L) \cdot \lambda}{M_0 \cdot \tau \cdot e^{-\frac{TI}{T_{1B}}} \cdot (1 - e^{-\frac{T_{sat}}{T_{1B}}}) \cdot e^{-\frac{2 \cdot TE_{label}}{T_{2B}}} \cdot \alpha} \quad [1]$$

where $C$, $L$, and $M_0$ are the signal intensities in the control, labeled, and proton-density images, $\lambda$ is the tissue-blood partition coefficient [0.9 ml/g that has been used for abdominal tissues (31, 32)], $\tau$ is the time between the first and second VS labeling pulses, $TI$ is the time between the first VS labeling and image acquisition, $T_{sat}$ is the time between global saturation and first VS labeling pulses, $T_{1B}$ is $T_1$ of blood [1350 ms at 1.5 T (5)], $TE_{label}$ is the duration of VS labeling, $T_{2B}$ is $T_2$ of blood [290 ms at 1.5 T (33)], and $\alpha$ represents the total inversion efficiency of four adiabatic inversion pulses in background suppression [0.75 (34)]. The placenta was manually segmented on proton-density images of the subject, and global placental perfusion was calculated by averaging perfusion of all voxels within the placenta of each subject. For multiple placental ASL scans that were performed consecutively in each subject as described below, identical segmentation of the placenta was used to avoid changes in placental perfusion measurement due to inconsistent segmentation.

## Experimental Setup

All scans were performed on a GE MR450 1.5 T scanner (GE Healthcare, Waukesha, WI, USA) with gradients supporting Gmax of 50 mT/m and slew rate of 200 mT/m/ms. The body coil and an eight-channel phased array cardiac coil were used for RF transmission and reception, respectively. In this study, only healthy pregnant volunteers with a normal prenatal history and normal ultrasound screening/biometry were recruited during their second or third trimester of pregnancy. Exclusion criteria included multiple gestation pregnancies, congenital infection, and documented chromosomal abnormalities. Subjects were scanned either in the supine or lateral decubitus position depending on the subject size and their preference. This study was approved by the institutional review board of Children's National Medical Center. All pregnant volunteers provided written consent in accordance with institutional policy.

## Comparison with PCASL

Placental VSASL and PCASL scans were performed consecutively in seven healthy pregnant volunteers [gestational age (GA) at MRI = 25.4 ± 4.7; range 21.9 – 35.4 weeks]. These two imaging sequences shared the identical image acquisition described above. PCASL was performed twice with two different labeling positions; the labeling plane was placed 2.2 cm above and below the axial imaging slab for each case, avoiding an overlap between imaging slab and labeling plane. In the former case, the labeling plane was placed in the descending aorta perpendicular to the blood flow in it. While this would label all arterial blood flowing into the placenta, the labeling plane may be too far from the placenta leading to ASL signal loss. In the latter case, the labeling plane was presumably placed near the uterine arteries thus being closer to the placenta; however the labeling plane may be even lower than the uterine arteries depending on the location of the placenta, resulting in almost no labeling. Other imaging parameters of PCASL included labeling duration = 1450 ms,

post-labeling delay = 2025 ms, TR = 4837 ms, and NEX = 3. Background suppression was achieved using one saturation and five inversion pulses at 4322, 3510, 2005, 903, 325, and 73 ms prior to image acquisition, respectively. Total scan time was 4:20 min. Perfusion quantification of PCASL data was performed using the standard method described in Ref. 5 and 14.

## Reproducibility

To test reproducibility, placental VSASL scan was repeated back to back within the same scan session without repositioning of the subject in fourteen healthy pregnant volunteers (GA at MRI = 27.8 ± 5.3; range 21.4 – 35.4 weeks). A rank correlation coefficient, Kendall's $\tau$ was calculated to verify that the within-subject difference was independent of the within-subject mean (35). Reproducibility was then assessed using the following parameters that are commonly used in other studies (36-41).

1. Within-subject standard deviation(wsSD) $\sqrt{mean(SD^2)} = \sqrt{\sum_{k=1}^{n}(x_k - y_k)^2/2n}$ where $SD$ is the standard deviation of the two measurements, $x_k$ and $y_k$ of the $k^{th}$ subject among total of $n$ subjects (35).
2. Within-subject coefficient of variation (wsCV) was calculated using two approaches by using wsCV $\sqrt{mean(CV^2)}$ where $CV$ is the coefficient of variation of each subject and by using wsCV = wsSD/μ where μ is the overall mean of all repetitions and subjects (35).
3. Repeatability =√2×1.96×wsSD. The difference between the repeated measurements for the same subject was expected to be less than this interval with a probability of 95% (35).
4. Intraclass correlation coefficient (ICC) was calculated using the two-way mixed-effect model as follows.

$$ICC = \frac{MSB - MSE}{MSB + (k-1)\cdot MSE} \quad [2]$$

where $MSB$ is the mean square between-subject error and $MSE$ is the mean square error. ICC ranges from 0–1, and values closer to 1 indicate higher reliability (42).

## Response to Maternal Hyperoxia

Maternal hyperoxia was employed to modulate VSASL signal in the placenta. Changes in placental VSASL signal with hyperoxia do not necessarily indicate changes in placental perfusion because apparent ASL signal is also a function of $T_1$ of blood, which decreases with increased oxygenation in the blood. Nevertheless, by showing alteration in VSASL signal inflow-dependence can be demonstrated. Maternal hyperoxia was induced by allowing 100% oxygen (15 L/min) into the facial oxygen mask (Ceretec, Inc. Garden Grove, CA) worn by the subject. Placental VSASL with hyperoxia was performed in seven healthy

pregnant women (GA at MRI = 30.4 ± 5.7; range 21.4 – 35.4 weeks) using two slightly different schemes. In three subjects, oxygen was inhaled for 4 min and was stopped immediately before the placental VSASL scan started. In remaining four subjects, oxygen inhalation was started 2 min prior to the start of VSASL scan and was maintained during the VSASL scan (i.e. oxygen inhalation for 5:55 min). These seven subjects were a subset of subjects in the reproducibility test described above, and in these subjects the experiment with hyperoxia was performed immediately after the reproducibility test. Quantification of VSASL with hyperoxia was performed using proton-density images acquired before oxygen inhalation in order to avoid the effect of $T_1$ change of the placenta under hyperoxia.

### Varying Cutoff Velocity

Three placental VSASL scans were performed using cutoff velocity of 2 cm/s, 4cm/s and infinity (i.e. no labeling). Larger cutoff velocity is expected to generate the label farther from the imaging region, leading to reduced apparent VSASL signal. However, because one can argue that these apparent ASL signal changes are due to different sensitivity to subject breathing motion rather than to blood flow, 2D VSASL was also performed in the same subjects to demonstrate that the contribution of subject motion to VSASL signal is not significant. This 2D VSASL sequence used the same VS labeling pulse as in the proposed 3D VSASL, but used 2D multislice single-shot spiral imaging, which acquires ASL images of the whole imaging region every TR unlike the segmented imaging in 3D VSASL. The sequence was performed using an interleaved scheme of three different TRs with cutoff velocity of 2 cm/s, 4 cm/s, and infinity (i.e. order of TRs: $TR_1$–$TR_2$–$TR_3$–$TR_1$–$TR_2$–$TR_3$-… where $TR_1$, $TR_2$, $TR_3$ are the TRs with cutoff velocity of 2 cm/s, 4cm/s and infinity, respectively). The total number of TRs in this scan was 90 and the number of labeled images with each cutoff velocity was 30. For data analysis, a small ROI was segmented in the middle of the placenta on a selected slice such that the ROI remained within the placenta across time series in the presence of misregistration due to subject motion. Average labeled signal in the ROI was measured for each TR, and the time series of the average signal were grouped separately for each cutoff velocity. Temporal standard deviation (SD) of the labeled signal for each cutoff velocity was then calculated. The time series of average signal can be modeled as a sum of perfusion-related constant signal and two random variables, $N_p$ and $N_m$ where $N_p$ represents the physiological noise that would be observed if conventional ASL methods were applied, and $N_m$ represents the noise due to signal reduction caused by subject motion at the time of VS labeling. Because these two random variables are uncorrelated, the overall temporal SD of the labeled signal, $\sigma$ can be expressed as $\sigma = \sqrt{\sigma_p^2 + \sigma_m^2}$ where $\sigma_p$ and $\sigma_m$ are the SD of $N_p$ and $N_m$ respectively. Temporal SDs with three different cutoff velocities were compared to each other to determine whether $\sigma$ decreased as $\sigma_m$ decreased by raising cutoff velocity. No significant difference in $\sigma$ was expected between different cutoff velocities if $\sigma_m$ was negligible compared to $\sigma_p$. Other imaging parameters for 2D VSASL included TE/TR = 16/5000 ms, TI = 1630 ms, FOV = 360–380 cm, matrix size = 64 × 64, 6-mm slice thickness with 2-mm slice gap, and number of slices = 12. Background suppression was achieved using one saturation and two inversion sech pulses placed at 4453, 1620, and 410 ms prior to image acquisition respectively. Total scan time of 2D interleaved

VSASL was 8:04 min. This experiment was performed in six healthy pregnant women (GA at MRI = 32.2 ± 2.3; range 28.3 – 34.4 weeks).

## Results

### Comparison with PCASL

Figure 1 shows the apparent placental perfusion measured using VSASL and PCASL with the labeling planes above and below the imaging slab. Apparent placental perfusion was significantly higher with VSASL than either PCASL method using a paired t-test ($p < 0.01$ for both). The ratio of apparent placental perfusion measured using PCASL to VSASL was 16 ± 12% and 9 ± 11% with upper and lower labeling planes, respectively. PCASL with two different labeling locations showed different patterns of perfusion for each subject, depending on the location of the placenta in the uterus. In Subject 1–4, the placenta was located at a relatively lower position in the uterus and the apparent placental perfusion signal was higher with the upper labeling plane versus lower labeling. In Subject 5–7, the placenta was located at a relatively higher position in the uterus and the apparent placental perfusion was higher with the lower labeling plane versus upper labeling. Figure 2 compares ASL images measured using different labeling approaches in Subject 4 and 6 from Figure 1, whose placenta was located lower and higher in the uterus respectively. In each subject, all ASL scans used the same prescan parameters and all ASL images are windowed identically. Both subjects exhibited lobulated patterns of perfusion signal when ASL SNR was adequate. It can be seen that in the PCASL images, only the regions inside the lobules showed high ASL signal whereas in the VSASL images, regions outside the lobules showed a fair amount of ASL signal in addition to high signal inside the lobules. This was the major contribution to the difference in apparent placental perfusion between VSASL and PCASL.

### Reproducibility

Correlation and Bland-Altman plots of the two, repeated VSASL scans are shown in Figure 3. Kendall's $\tau$ was found to be 0.12 ($p = 0.59$) and confirmed that there was no significant correlation between the difference and magnitude of the placental perfusion measurements. Placental VSASL demonstrated high reproducibility based on the following metrics: wsSD = 7.1 ml/100 g/min (note that overall mean of placental perfusion in this experiment was 195 ml/100 g/min); wsCV was found to be 3.4% by using the root mean square approach and 3.6% by dividing wsSD by overall mean; repeatability = 19.7 ml/100 g/min; ICC = 0.97.

### Response to Maternal Hyperoxia

Figure 4 compares the apparent placental perfusion in response to maternal hyperoxia with the placental perfusion measurements from the reproducibility test. Subject 1–3 inhaled 100% oxygen for 4 min and Subject 4–7 inhaled for 5:55 min as described above. In both schemes of inhalation, apparent placental perfusion either increased or decreased with hyperoxia for each subject. The change in placental perfusion between the two repeated measurements under normoxia was -0.2 ± 2.8% and the change between normoxia and hyperoxia (i.e. between ‘VSASL repeat’ and ‘VSASL hyperoxia’ denoted in Figure 4) was -1.9 ± 16.6%. There was no significant difference between these three placental perfusion measurements; however, absolute difference in apparent placental perfusion between

normoxia and hyperoxia was significantly larger than that of two repeated measurements under normoxia ($p < 0.01$). Representative VSASL images from two subjects are demonstrated in Figure 5. Again, in each subject, all three VSASL scans used the same prescan parameters and all three VSASL images are windowed identically.

### Varying Cutoff Velocity

Figure 6 shows the apparent placental perfusion measured using VSASL with cutoff velocity of 2 cm/s, 4 cm/s, and infinity. The differences between three measurements were all statistically significant ($p < 0.01$ for all). With respect to the placental perfusion measured with cutoff velocity of 2 cm/s (default for all other experiments in this study), the ratio of apparent placental perfusion measured with cutoff velocity of 4 cm/s and infinity was 71.2 ± 15.1% and 0.2 ± 3.5%, respectively. This demonstrated that apparent placental perfusion was reduced as cutoff velocity increased as expected. In the same subjects, interleaved 2D placental VSASL scan was successfully performed, with mild misregistration between time series. The area of ROI segmented in the placenta was 10.2 ± 4.3 $cm^2$. The temporal SD of average labeled signal in the ROI was calculated for each cutoff velocity and was normalized by proton-density signal for comparison between subjects (see Figure 7). There was no statistically significant difference in the temporal SD between the three cutoff velocities ($p > 0.1$ for all), which confirmed that contribution of subject motion to VSASL signal was not significant.

## Discussion

This study demonstrates the feasibility of non-invasive placental perfusion imaging using VSASL. In our results, VSASL showed markedly enhanced average ASL signal within the placenta compared to PCASL mostly due to the increased ASL signal outside the lobules. Placental VSASL also showed high reproducibility, despite the intrinsically large motion of the placenta and a labeling method that is sensitive to it. Lastly, placental VSASL demonstrated the dependence on blood inflow by responding to 100% oxygen inhalation and varying cutoff velocity. In keeping with our previous study, where placental perfusion measured in healthy pregnancies using VSASL was consistent with the literature values of total placental volume flow based on ultrasound (20), this study supports the feasibility of placental VSASL for quantifying meaningful perfusion signal in the human placenta.

The biggest difference of our approach from the previous placental ASL studies is the use of VSASL, which enabled the whole placenta coverage with adequate ASL signal in the placenta. While those early studies deployed the FAIR technique from brain ASL, the current standard ASL method in the brain is PCASL, which was introduced relatively recently (6). Therefore, it seemed appropriate to compare VSASL with PCASL for placental perfusion imaging because at minimum PCASL is expected to achieve higher SNR than FAIR. In our results, VSASL demonstrated significantly higher ASL signal within the placenta than PCASL. This was mainly because of the considerable ASL signal outside of the lobules on the VSASL images. As demonstrated in pregnant rhesus macaque using contrast agent in Ref. 43, these regions outside the lobules show far longer arterial transit delay compared to the regions inside the lobules. Although PCASL showed brighter signal

than VSASL inside the lobules where arterial transit delay is likely shorter than the post-labeling delay (Subject 4 with PCASL upper label and Subject 6 with PCASL lower label in Figure 1), PCASL showed near-zero signal outside the lobules presumably due to very long transit delay of arterial blood, resulting in significantly lower global placental perfusion measurements compared to VSASL.

While VSASL demonstrated significantly higher ASL signal than PCASL with either labeling location, comparison of PCASL data between these two labeling locations provides further insight into arterial blood path to the placenta. In the subjects with the placenta located relatively lower in the uterus, PCASL with lower labeling showed almost zero ASL signal probably because the labeling plane was located even lower than the uterine arteries where blood flow changes its direction from downward to slightly upward. Using upper labeling in these subjects, ASL signal was much higher because the arterial blood labeled in the descending aorta is likely to arrive at the placenta in a relatively short time. On the other hand, in the subjects with the relatively higher placenta, lower labeling generated higher ASL signal than upper labeling. It can be speculated that this is because the lower labeling plane was closer to the imaging region. However, the labeling efficiency of lower labeling plane in this case may be compromised because the velocity of blood flow at this level may be slower than the range of target velocity of pseudocontinuous labeling pulse and/or because blood flow may be labeled twice (firstly in the descending aorta and secondly in the uterus), negating the labeling effect. Again, VSASL generated sufficient perfusion signal in the placenta regardless of the location of the placenta, without the need to determine the labeling location.

The reproducibility of proposed placental VSASL was found to be high. Previous studies have demonstrated reproducibility of brain ASL within the same day, despite the use of different labeling schemes between studies (36,37,41). Floyd et al. found that wsSD was 3.0 ml/100 g/min and wsCV was 5.8% in their study using two ASL scans from separate imaging sessions one hour apart. Jahng et al. showed that wsCV was 1 – 6% and ICC was 0.78 – 0.81 within a single two-hour imaging session, using a few different ASL methods. Henriksen et al. demonstrated wsSD of 1.8 ml/100 g/min and wsCV of 4.8% using two ASL scans performed within a single imaging session of 90 min. Our results demonstrated a slightly higher reproducibility compared to these values. While this may be attributed in part to the fact that the placental VSASL scan was repeated back to back without repositioning of the subjects in our study, this confirms the high precision of the proposed measurement technique when physiological and environmental variations are minimized.

In this study, two experiments were performed to modulate ASL signal, thereby demonstrating inflow-dependence of placental VSASL signal. One way of modulating ASL signal was to utilize maternal hyperoxia induced by inhalation of 100% oxygen. Similar studies with a hyperoxia challenge have been performed in brain ASL (44 – 47). With 100% oxygen, these prior studies reported approximately a 20% decrease in ASL signal in the gray matter, which is most likely due to reduced $T_1$ of blood caused by increased concentration of dissolved oxygen in the plasma, which acts as a weak paramagnetic contrast agent (45). After compensation for reduced $T_1$, they demonstrated a 2 – 7% decrease in CBF in the same regions. On the basis of Eq. 1 and literature values of $T_1$ of blood at 1.5 T during

normoxia and hyperoxia (48,49), blood $T_1$ change with 100% oxygen is expected to cause approximately a 10% decrease in our placental VSASL signal. However, another factor that must be considered in VSASL is the increased $T_2$ of blood due to reduced deoxyhemoglobin under hyperoxia (50), given that in VSASL, $T_2$ decay also occurs in the label during the two VS labeling pulses as shown in Eq. 1 (total duration: 2 × 21 ms = 42 ms). This effect alone is expected to cause a 7% increase in VSASL signal. Combining these two factors, the overall change in VSASL signal may be positive or negative depending on the actual amount of $T_1$ reduction and $T_2$ increase in each subject. This may explain inconsistent changes in apparent placental perfusion between subjects in our results. Nevertheless, the absolute change in apparent placental perfusion with hyperoxia was significantly larger than those of repeatability test, which demonstrates that placental VSASL signal is dependent on blood inflow.

The other method used to modulate VSASL signal in this study was to vary cutoff velocity. As expected, our data showed that apparent placental perfusion significantly decreased with increasing cutoff velocity given that increasing cutoff velocity has the effect of generating the label more distant from the imaging region. Although not practical for placental perfusion measurement because of low SNR and suboptimal background suppression, 2D VSASL with single-shot imaging was performed to confirm that contribution of subject respiratory motion to VSASL signal is not significant. Compared to control images (i.e. images without label), labeled images in VSASL contain signal reduction contributed by any moving sources, such as blood flow (i.e. contribution of true perfusion) and subject motion. Because the VS labeling pulse was not gated to respiration of subject, the additional signal reduction due to respiratory motion must vary across time series of 2D VSASL. This can be considered a noise distribution with a non-zero mean and SD proportional to the mean. Cutoff velocity in 2D VSASL was changed to vary the SD of this noise, but there was no significant difference in the overall SD, demonstrating that the SD of this noise is negligible compared to the SD of the baseline physiological noise and therefore the mean of this noise is also negligible.

Given that presently there exists no gold-standard method for measuring perfusion of the human placenta in vivo, direct validation against a ground truth is complicated. Therefore, this study was designed to provide evidences supporting the use of VSASL to evaluate placental perfusion. A definitive validation of placental VSASL is still warranted and may be performed using a gold standard perfusion measurement technique such as positron emission tomography (PET) or radioactive microspheres in animal models.

In the setup of VSASL, one important parameter is cutoff velocity. Given that VSASL perfusion is measured based on the amount of blood flow that decelerates from above this velocity to below this velocity, this value must match blood velocity in the small arterial vessels that are very close to or within imaging voxels. The typical value for the cutoff velocity in brain VSASL is 2 cm/s on the basis of blood velocity measured in the arterioles of the cortical regions (21,22). In the placenta of normal pregnancies, Kurjak et al. (51) reported maximum velocity of blood ranging from 25 to 37 cm/s in the intervillous space in all three trimesters, and Alouini et al. (52) and Mäkikallio et al. (53) found maximum blood velocity of 3 – 5 cm/s in the intervillous space in the first trimester. While Kurjak et al. (51)

reported markedly higher blood velocity than the other two studies, in either case, 2 cm/s seems acceptable for the cutoff velocity of placental VSASL even after converting maximum velocity to mean velocity on the assumption of laminar flow, which likely holds true for these low velocity ranges. Furthermore, in the setting of placental dysfunction, blood velocity in the placenta may differ from normal pregnancy. While Mäkikallio et al. (53) found no significant difference in blood velocity in intervillous space between healthy pregnancies and pregnancies complicated by preeclampsia, further investigation of optimal cutoff velocity may be required in other pathological conditions of the placenta.

Another parameter setup in VSASL that may affect perfusion measurement is the direction of velocity encoding. Wong et al. demonstrated that CBF measured using VSASL becomes isotropic with respect to encoding direction for lower cutoff velocity, all comparable to CBF measurement from conventional ASL (21). This is in large part because of the tortuosity of small arterioles in the brain. Similarly, in the placenta, maternal arterial blood that is delivered from the spiral artery to the central cavity of the intervillous space disperses radially (i.e. in all directions) between the fetal villous trees, which also provide the tortuous path for fetal blood inflow (54). We postulate that placental VSASL exhibits no significant sensitivity to velocity encoding direction; however this remains to be validated in future work.

ASL imaging (in any organs) during pregnancy may require knowledge of altered relaxation times of blood or separate measurements of relaxation times in each subject for accurate quantification, regardless of the labeling method. Despite no available literature on direct measurement of blood $T_1$, reduced hematocrit in pregnancy [from 40% to 35% (55)] likely increases $T_1$ of maternal blood. $T_1$ of fetal blood is also expected to be longer than that of adults due to the presence of fetal hemoglobin (56). Notably, overestimation of placental perfusion due to altered relaxation times was calculated to be much lower with VSASL (including longer $T_2$ effect) than PCASL (approximately 6% versus 11%) in our current imaging protocol.

Although we successfully demonstrated the feasibility of placental VSASL, the current setup of VSASL may be further optimized for placental perfusion imaging. First, our dual sech VS labeling pulse may be replaced by BIR-8 based pulses to reduce sensitivity to increased B1 inhomogeneity in the abdomen (23,24). This will improve labeling efficiency of VSASL and the benefit will be even higher at higher field strengths. Second, the current axial orientation of the imaging slab can be changed to oblique orientation such that the short axis of the placenta can be aligned with the through-plane direction, leading to reduction of the number of slices and therefore reduction of scan time. Lastly, despite the pros and cons of long/short TI in VSASL (57), theoretically optimal TI for maximal SNR corresponds to $T_1$ of blood, which is 1350 ms at 1.5 T. Reduced TI will also reduce the scan time and may be beneficial for reducing the potential error from short MTT of the placenta. However, the estimated SNR loss due to the current, longer TI (1600 ms) is less than 2%. These optimizations are currently underway.

## Conclusion

We have demonstrated the feasibility of non-invasive placental perfusion imaging using VSASL, which enabled whole placenta coverage with enhanced SNR. Placental VSASL generated significantly higher ASL signal than PCASL and showed high reproducibility within the same imaging session. Also, placenta VSASL was found to be dependent on blood inflow based on modulation of VSASL signal using 100% oxygen inhalation and variation of cutoff velocity. This study supports the use of VSASL in placental perfusion imaging and provides a framework for future investigation of placental perfusion imaging in pregnancies complicated by placental insufficiency such as FGR and preeclampsia.

## Acknowledgments

We thank the healthy pregnant volunteers for their participation in this study. This study was supported by R01 HL116585-01 from NIH National Heart, Lung, and Blood Institute, and UL1TR000075 and KL2TR000076 from the NIH National Center for Advancing Translational Sciences.

## References

1. Krishna U, Bhalerao S. Placental insufficiency and fetal growth restriction. J Obstet Gynaecol India. 2011; 61:505–511. [PubMed: 23024517]
2. Gardosi J. Clinical strategies for improving the detection of fetal growth restriction. Clin Perinatol. 2011; 38:21–31. [PubMed: 21353087]
3. Roberts JM, Bell MJ. If we know so much about preeclampsia, why haven't we cured the disease? J Reprod Immunol. 2013; 99:1–9. [PubMed: 23890710]
4. Pauli JM, Repke JT. Preeclampsia Short-term and Long-term Implications. Obstet Gynecol Clin North Am. 2015; 42:299–313. [PubMed: 26002168]
5. Alsop DC, Detre JA, Golay X, Günther M, Hendrikse J, Hernandez-Garcia L, Lu H, Macintosh BJ, Parkes LM, Smits M, van Osch MJ, Wang DJ, Wong EC, Zaharchuk G. Recommended implementation of arterial spin-labeled perfusion MRI for clinical applications. Magn Reson Med. 2015; 73:102–116. [PubMed: 24715426]
6. Dai W, Garcia D, de Bazelaire C, Alsop DC. Continuous flow-driven inversion for arterial spin labeling using pulsed radio frequency and gradient fields. Magn Reson Med. 2008; 60:1488–1497. [PubMed: 19025913]
7. Kwong KK, Chesler DA, Weisskoff RM, Donahue KM, Davis TL, Ostergaard L, Campbell TA, Rosen BR. MR perfusion studies with T1-weighted echo planar imaging. Magn Reson Med. 1995; 34:878–887. [PubMed: 8598815]
8. Kim SG. Quantification of regional cerebral blood flow change by flow-sensitive alternating inversion recovery (FAIR) technique: application to functional mapping. Magn Reson Med. 1995; 34:293–301. [PubMed: 7500865]
9. Zun Z, Wong EC, Nayak KS. Assessment of myocardial blood flow (MBF) in humans using arterial spin labeling (ASL): feasibility and noise analysis. Magn Reson Med. 2009; 62:975–983. [PubMed: 19672944]
10. Zhang JL, Morrell G, Rusinek H, Sigmund EE, Chandarana H, Lerman LO, Prasad PV, Niles D, Artz N, Fain S, Vivier PH, Cheung AK, Lee VS. New magnetic resonance imaging methods in nephrology. Kidney Int. 2014; 85:768–778. [PubMed: 24067433]
11. Martirosian P, Boss A, Schraml C, Schwenzer NF, Graf H, Claussen CD, Schick F. Magnetic resonance perfusion imaging without contrast media. Eur J Nucl Med Mol Imaging. 2010; 37(1):S52–64. [PubMed: 20461372]
12. Bucklin, BA., Baysinger, CL., Gambling, DA. Practical Approach to Obstetric Anesthesia. 2nd. Lippincott Williams and Wilkins; 2016.
13. Gowland P. Placental MRI. Semin Fetal Neonatal Med. 2005; 10:485–90. [PubMed: 16027055]

14. Buxton RB, Frank LR, Wong EC, Siewert B, Warach S, Edelman RR. A general kinetic model for quantitative perfusion imaging with arterial spin labeling. Magn Reson Med. 1998; 40:383–396. [PubMed: 9727941]
15. Guo, J., Wong, EC. Proceedings of the 21st Annual Meeting of ISMRM. Salt Lake City, Utah, USA: 2013. Pulmonary Blood Flow Measurement using Velocity-Selective Arterial Spin Labeling at 3.0T. Abstract 2149
16. Gowland PA, Francis ST, Duncan KR, Freeman AJ, Issa B, Moore RJ, Bowtell RW, Baker PN, Johnson IR, Worthington BS. In Vivo Perfusion Measurements in the Human Placenta Using Echo Planar Imaging at 0.5 T. Magn Reson Med. 1998; 40:467–473. [PubMed: 9727951]
17. Duncan KR, Gowland P, Francis S, Moore R, Baker PN, Johnson IR. The Investigation of Placental Relaxation and Estimation of Placental Perfusion Using Echo-planar Magnetic Resonance Imaging. Placenta. 1998; 19:539–543. [PubMed: 9778128]
18. Francis ST, Duncan KR, Moore RJ, Baker PN, Johnson IR, Gowland PA. Non-invasive mapping of placental perfusion. Lancet. 1998; 351:1397–1399. [PubMed: 9593410]
19. Derwig I, Lythgoe DJ, Barker GJ, Poon L, Gowland P, Yeung R, Zelaya F, Nicolaides K. Association of placental perfusion, as assessed by magnetic resonance imaging and uterine artery Doppler ultrasound, and its relationship to pregnancy outcome. Placenta. 2013; 34:885–891. [PubMed: 23937958]
20. Zun Z, Zaharchuk G, Andescavage NN, Donofrio MT, Limperopoulos C. Non-Invasive Placental Perfusion Imaging in Pregnancies Complicated by Fetal Heart Disease Using Velocity-Selective Arterial Spin Labeled MRI. Sci Rep. 2017; 7:16126. [PubMed: 29170468]
21. Wong EC, Cronin M, Wu WC, Inglis B, Frank LR, Liu TT. Velocity-Selective Arterial Spin Labeling. Magn Reson Med. 2006; 55:1334–1341. [PubMed: 16700025]
22. Qiu D, Straka M, Zun Z, Bammer R, Moseley ME, Zaharchuk G. CBF measurements using multidelay pseudocontinuous and velocity-selective arterial spin labeling in patients with long arterial transit delays: comparison with xenon CT CBF. J Magn Reson Imaging. 2012; 36:110–119. [PubMed: 22359345]
23. Meakin JA, Jezzard P. An optimized velocity selective arterial spin labeling module with reduced eddy current sensitivity for improved perfusion quantification. Magn Reson Med. 2013; 69:832–838. [PubMed: 22556043]
24. Guo J, Meakin JA, Jezzard P, Wong EC. An optimized design to reduce eddy current sensitivity in velocity-selective arterial spin labeling using symmetric BIR-8 pulses. Magn Reson Med. 2015; 73:1085–1094. [PubMed: 24710761]
25. Manganaro L, Fierro F, Tomei A, La Barbera L, Savelli S, Sollazzo P, Sergi ME, Vinci V, Ballesio L, Marini M. MRI and DWI: feasibility of DWI and ADC maps in the evaluation of placental changes during gestation. Prenat Diagn. 2010; 30:1178–1184. [PubMed: 21064115]
26. Bonel HM, Stolz B, Diedrichsen L, Frei K, Saar B, Tutschek B, Raio L, Surbek D, Srivastav S, Nelle M, Slotboom J, Wiest R. Diffusion-weighted MR imaging of the placenta in fetuses with placental insufficiency. Radiology. 2010; 257:810–819. [PubMed: 21084415]
27. Morita S, Ueno E, Fujimura M, Muraoka M, Takagi K, Fujibayashi M. Feasibility of diffusion-weighted MRI for defining placental invasion. J Magn Reson Imaging. 2009; 30:666–671. [PubMed: 19711415]
28. Pruessmann KP, Weiger M, Scheidegger MB, Boesiger P. SENSE: Sensitivity encoding for fast MRI. Magn Reson Med. 1999; 42:952–962. [PubMed: 10542355]
29. Roemer PB, Edelstein WA, Hayes CE, Souza SP, Mueller OM. The NMR phased array. Magn Reson Med. 1990; 16:192–225. [PubMed: 2266841]
30. Graves MJ, Emmens D, Lejay H, Hariharan H, Polzin J, Lomas DJ. T2 and T2* quantification using optimal B1 image reconstruction for multicoil arrays. J Magn Reson Imaging. 2008; 28:278–281. [PubMed: 18581394]
31. Robson PM, Madhuranthakam AJ, Dai W, Pedrosa I, Rofsky NM, Alsop DC. Strategies for reducing respiratory motion artifacts in renal perfusion imaging with arterial spin labeling. Magn Reson Med. 2009; 61:1374–1387. [PubMed: 19319891]

32. Bjornerud A, Johansson LO, Briley-Saebo K, Ahlstrom HK. Assessment of T1 and T2* effects in vivo and ex vivo using iron oxide nanoparticles in steady state–dependence on blood volume and water exchange. Magn Reson Med. 2002; 47:461–471. [PubMed: 11870832]
33. Stanisz GJ, Odrobina EE, Pun J, Escaravage M, Graham SJ, Bronskill MJ, Henkelman RM. T1, T2 relaxation and magnetization transfer in tissue at 3T. Magn Reson Med. 2005; 54:507–512. [PubMed: 16086319]
34. Garcia DM, Duhamel G, Alsop DC. Efficiency of inversion pulses for background suppressed arterial spin labeling. Magn Reson Med. 2005; 54:366–372. [PubMed: 16032674]
35. Bland JM, Altman DG. Measurement error. BMJ. 1996; 312:1654. [PubMed: 8664723]
36. Floyd TF, Ratcliffe SJ, Wang J, Resch B, Detre JA. Precision of the CASL-perfusion MRI technique for the measurement of cerebral blood flow in whole brain and vascular territories. J Magn Reson Imaging. 2003; 18:649–655. [PubMed: 14635149]
37. Jahng GH, Song E, Zhu XP, Matson GB, Weiner MW, Schuff N. Human brain: reliability and reproducibility of pulsed arterial spin-labeling perfusion MR imaging. Radiology. 2005; 234:909–916. [PubMed: 15734942]
38. Hermes M, Hagemann D, Britz P, Lieser S, Rock J, Naumann E, Walter C. Reproducibility of continuous arterial spin labeling perfusion MRI after 7 weeks. MAGMA. 2007; 20:103–115. [PubMed: 17429703]
39. Petersen ET, Mouridsen K, Golay X. The QUASAR reproducibility study,Part II: Results from a multi-center Arterial Spin Labeling test-retest study. Neuroimage. 2010; 49:104–113. [PubMed: 19660557]
40. Wang Y, Saykin AJ, Pfeuffer J, Lin C, Mosier KM, Shen L, Kim S, Hutchins GD. Regional reproducibility of pulsed arterial spin labeling perfusion imaging at 3T. Neuroimage. 2011; 54:1188–1195. [PubMed: 20800097]
41. Henriksen OM, Larsson HB, Hansen AE, Grüner JM, Law I, Rostrup E. Estimation of intersubject variability of cerebral blood flow measurements using MRI and positron emission tomography. J Magn Reson Imaging. 2012; 35:1290–1299. [PubMed: 22246715]
42. Shrout PE, Fleiss JL. Intraclass correlations: uses in assessing rater reliability. Psychol Bull. 1979; 86:420–428. [PubMed: 18839484]
43. Ludwig, KD., Fain, SB., Adamson, EB., Nguyen, S., Golos, TG., Reeder, SB., Bird, IM., Wieben, O., Shah, DM., Johnson, KM. Proceedings of the 4th Annual Meeting of HPP. Bethesda, MD, USA: 2017. Mapping the placental functional domains with ferumoxytol DCE MRI. abstract 10
44. Bulte DP, Chiarelli PA, Wise RG, Jezzard P. Cerebral perfusion response to hyperoxia. J Cereb Blood Flow Metab. 2007; 27:69–75. [PubMed: 16670698]
45. Zaharchuk G, Martin AJ, Dillon WP. Noninvasive imaging of quantitative cerebral blood flow changes during 100% oxygen inhalation using arterial spin-labeling MR imaging. AJNR Am J Neuroradiol. 2008; 29:663–667. [PubMed: 18397966]
46. Chiarelli PA, Bulte DP, Wise R, Gallichan D, Jezzard P. A calibration method for quantitative BOLD fMRI based on hyperoxia. Neuroimage. 2007; 37:808–820. [PubMed: 17632016]
47. Gauthier CJ, Hoge RD. Magnetic resonance imaging of resting OEF and $CMRO_2$ using a generalized calibration model for hypercapnia and hyperoxia. Neuroimage. 2012; 60:1212–1225. [PubMed: 22227047]
48. Tadamura E, Hatabu H, Li W, Prasad PV, Edelman RR. Effect of oxygen inhalation on relaxation times in various tissues. J Magn Reson Imaging. 1997; 7:220–225. [PubMed: 9039619]
49. Noseworthy MD, Kim JK, Stainsby JA, Stanisz GJ, Wright GA. Tracking oxygen effects on MR signal in blood and skeletal muscle during hyperoxia exposure. J Magn Reson Imaging. 1999; 9:814–820. [PubMed: 10373029]
50. Silvennoinen MJ, Clingman CS, Golay X, Kauppinen RA, van Zijl PC. Comparison of the dependence of blood R2 and R2* on oxygen saturation at 1.5 and 4.7 Tesla. Magn Reson Med. 2003; 49:47–60. [PubMed: 12509819]
51. Kurjak A, Dudenhausen JW, Hafner T, Kupesic S, Latin V, Kos M. Intervillous circulation in all three trimesters of normal pregnancy assessed by color Doppler. J Perinat Med. 1997; 25:373–380. [PubMed: 9350609]

52. Alouini S, Carbillon L, Perrot N, Uzan S, Uzan M. Intervillous and spiral artery flows in normal pregnancies between 5 and 10 weeks of amenorrhea using color Doppler ultrasonography. Fetal Diagn Ther. 2002; 17:163–166. [PubMed: 11914569]

53. Mäkikallio K, Jouppila P, Tekay A. First trimester uterine, placental and yolk sac haemodynamics in pre-eclampsia and preterm labour. Hum Reprod. 2004; 19:729–733. [PubMed: 14998978]

54. Burton GJ, Woods AW, Jauniaux E, Kingdom JC. Rheological and physiological consequences of conversion of the maternal spiral arteries for uteroplacental blood flow during human pregnancy. Placenta. 2009; 30:473–482. [PubMed: 19375795]

55. Abbassi-Ghanavati M, Greer LG, Cunningham FG. Pregnancy and laboratory studies: a reference table for clinicians. Obstet Gynecol. 2009; 114:1326–1331. [PubMed: 19935037]

56. Liu P, Chalak LF, Krishnamurthy LC, Mir I, Peng SL, Huang H, Lu H. T1 and T2 values of human neonatal blood at 3 Tesla: Dependence on hematocrit, oxygenation, and temperature. Magn Reson Med. 2016; 75:1730–1735. [PubMed: 25981985]

57. Zun Z, Hargreaves BA, Rosenberg J, Zaharchuk G. Improved multislice perfusion imaging with velocity-selective arterial spin labeling. J Magn Reson Imaging. 2015; 41:1422–1431. [PubMed: 24797337]

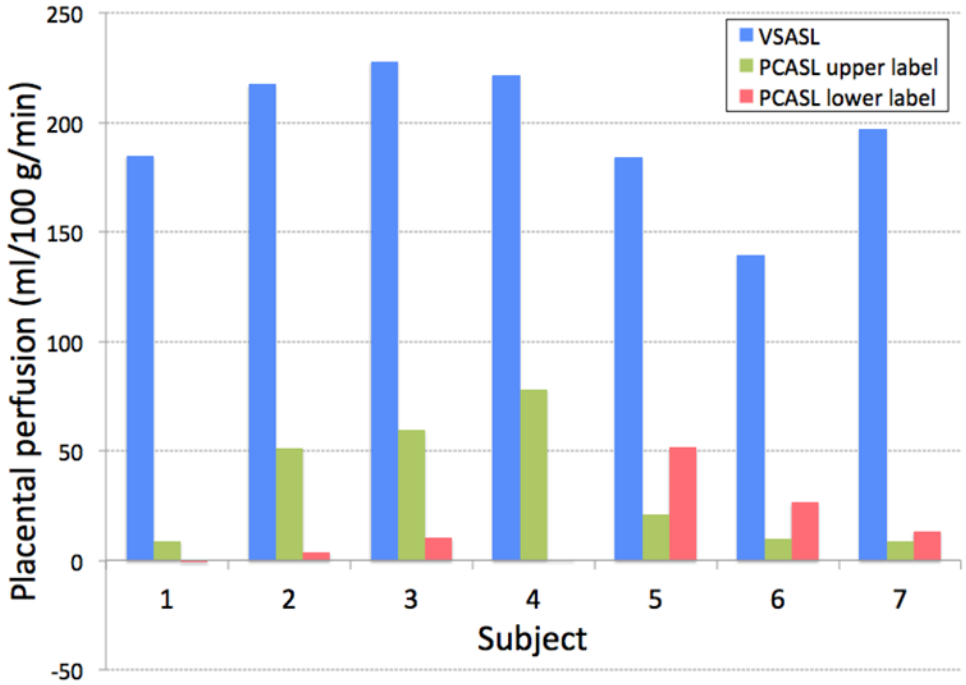


**Figure 1.**

Apparent placental perfusion measured using VSASL and PCASL with labeling plane above and below the imaging slab. VSASL showed dramatically higher perfusion measurement than either of PCASL methods in all subjects. With PCASL, upper labeling showed higher placental perfusion signal in the placenta that was located relatively lower in the uterus (Subject 1–4) and lower labeling showed higher placental perfusion signal in the placenta that was located relatively higher in the uterus (Subject 5–7).

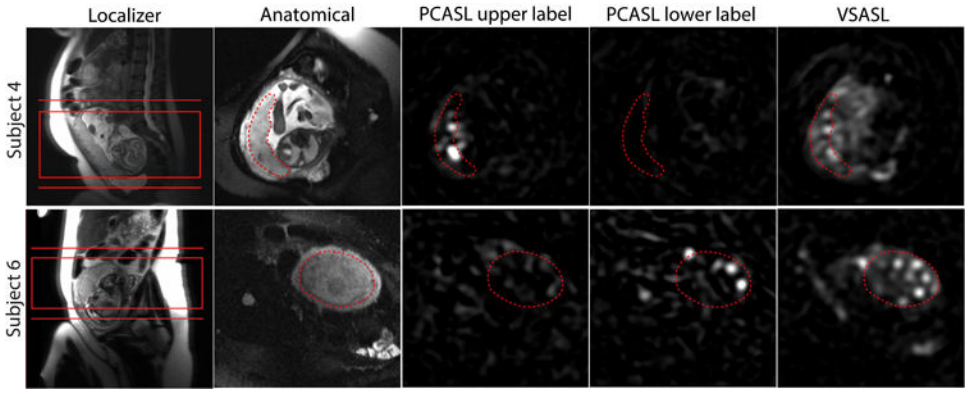


**Figure 2.**

Comparison of placental ASL images acquired using different labeling methods as well as localizer and anatomical images in Subject 4 and 6 from Figure 1. As shown in the localizer, the placenta was located relatively lower in Subject 4 and higher in Subject 6 inside the uterus. The common imaging slab of VSASL and PCASL and the two different locations of the labeling plane of PCASL are shown in the localizer images. In the other images, the placenta is delineated with the dotted line. PCASL signal in the placenta was higher with upper labeling in Subject 4 and with lower labeling in Subject 6, compared to the other location of the labeling plane. For both subjects, the average VSASL signal in the placenta was substantially higher than either PCASL scheme.

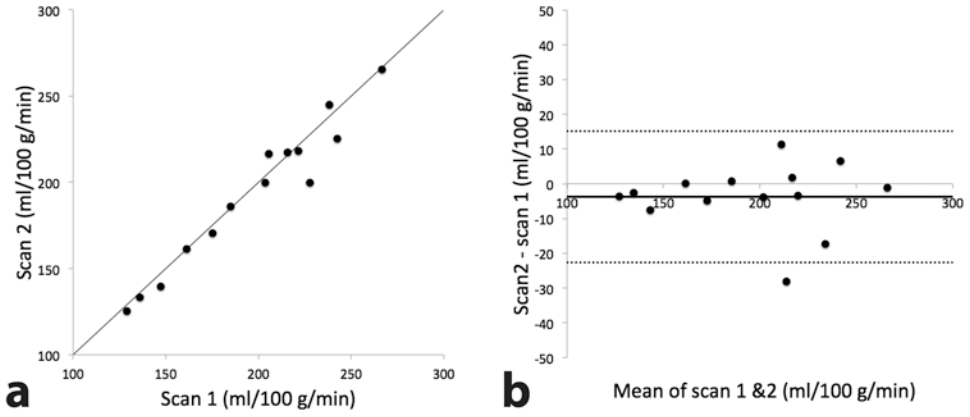


**Figure 3.**

Correlation (**a**) and Bland-Altman (**b**) plots of two repeated measurements of placental perfusion measured using VSASL back to back in the same scan session. In **b**, solid and dotted lines represent the mean difference and 95% limits of agreement respectively.

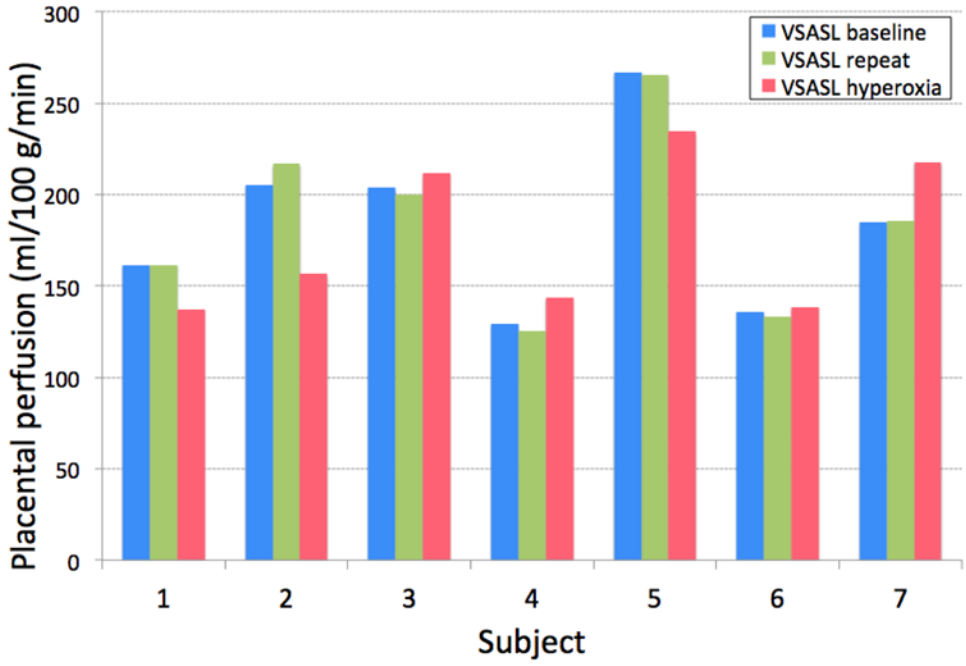


**Figure 4.**

Apparent placental perfusion in response to maternal hyperoxia induced by 100% oxygen inhalation, compared to the repeated measurements of placental perfusion before oxygen inhalation. During hyperoxia, apparent placental perfusion decreased in Subject 1, 2, and 5, and increased in the other subjects.

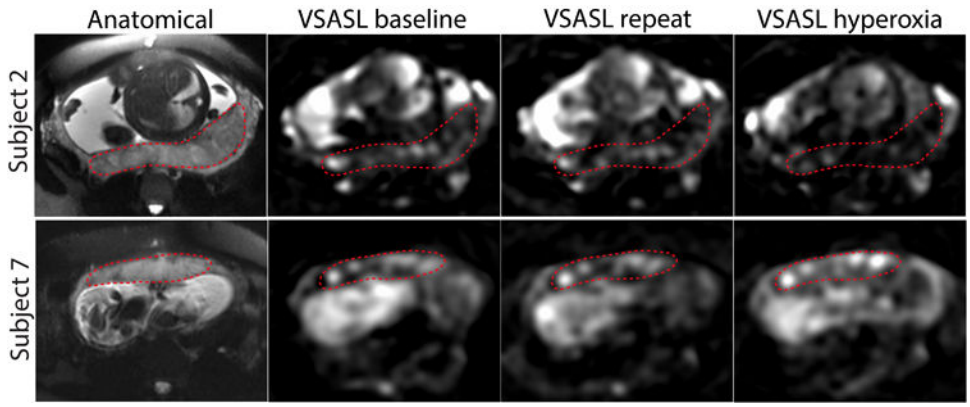


**Figure 5.**

Placental VSASL images of the reproducibility test (baseline, repeat) and hyperoxia scan acquired in Subject 4 and 7 from Figure 4. The placenta is delineated with the dotted line. While VSASL signal in the placenta was similar between the two scans before oxygen inhalation for both subjects, VSASL under hyperoxia demonstrated reduced signal in Subject 2 and increased signal in Subject 7 compared to their VSASL signal under normoxia.

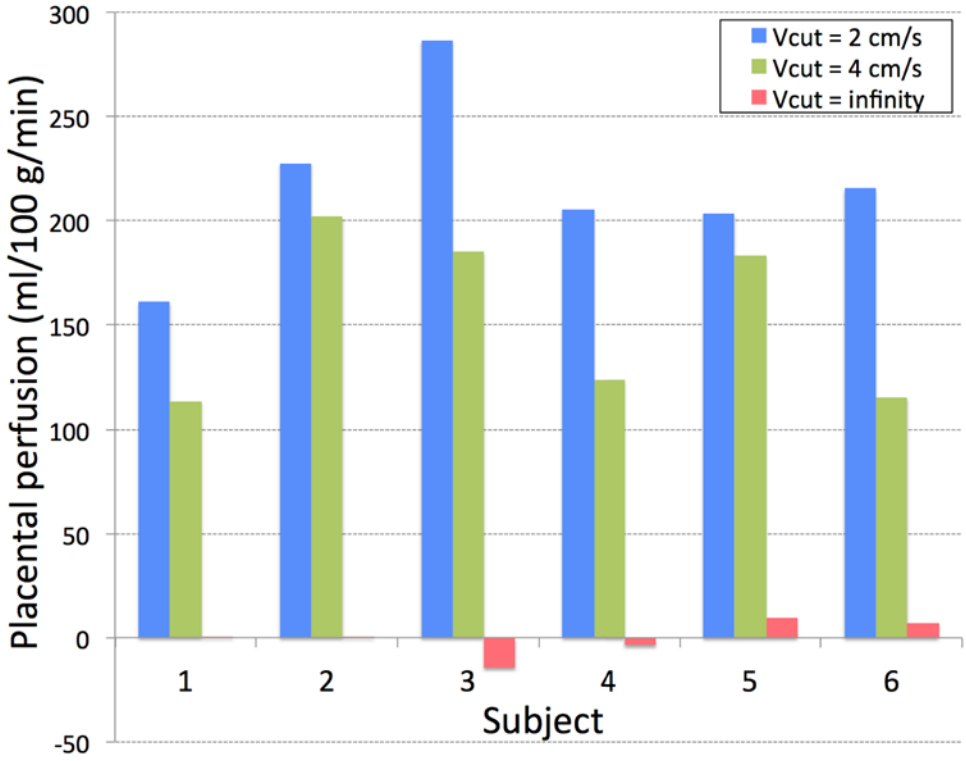


**Figure 6.**

Apparent placental perfusion measured using VSASL with cutoff velocity (Vcut) of 2 cm/s, 4 cm/s, and infinity (i.e.no labeling). Apparent placental perfusion was reduced significantly as cutoff velocity increased.

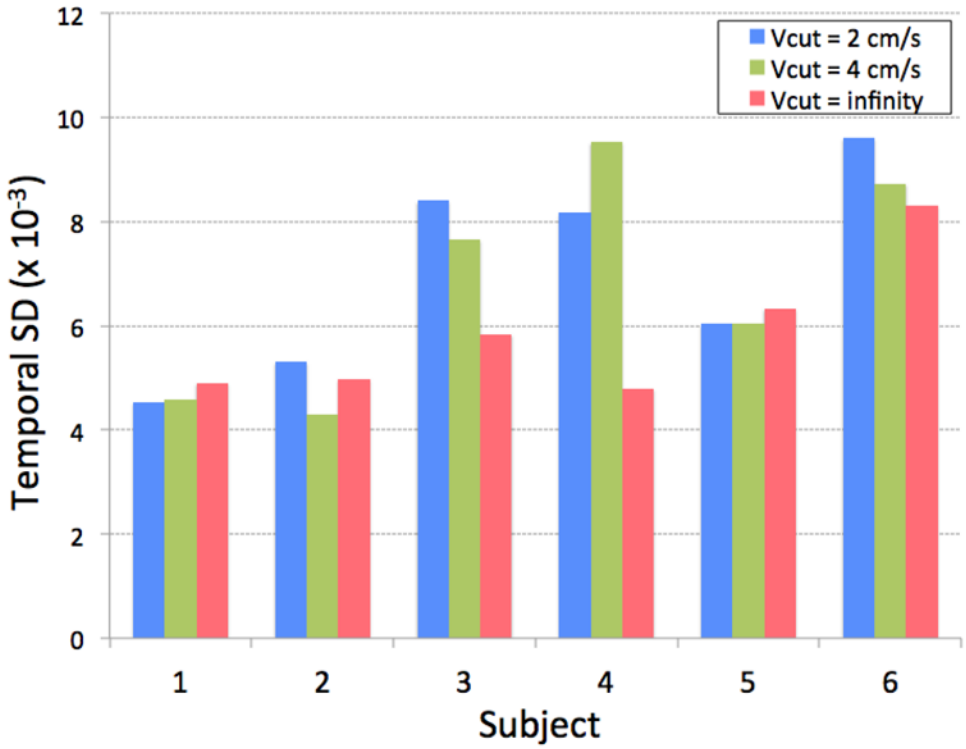


**Figure 7.**

Temporal standard deviation (SD) of 2D VSASL labeled signal time series in an ROI drawn within the placenta, with cutoff velocity of 2 cm/s, 4cm/s and infinity. No significant difference was present between the three cutoff velocities, confirming that contribution of subject motion to VSASL signal was not significant.